Annu. Rev. Nucl. Part. Sci. 1997. 47:359–94

THE QCD VACUUM AS AN INSTANTON LIQUID

E. Shuryak
Department of Physics, State University of New York, Stony Brook, New York 11794

T. Schäfer
Institute for Nuclear Theory, University of Washington, Seattle, Washington, 98195

KEY WORDS: hadronic structure, chiral symmetry, QCD correlation functions, QCD at finite temperature, QCD phase transitions

ABSTRACT

We review recent progress in understanding the importance of instanton effects in QCD. Instantons provide a mechanism for quark and gluon condensation, explain the $U(1)_A$ anomaly and the appearance of a non-perturbative vacuum energy density. In the framework of the instanton liquid model, a large number of hadronic correlation functions were calculated. The results are in good agreement with both experimental data and lattice simulations. We also review recent results on the phase structure of QCD-like theories. Instantons provide a mechanism for chiral symmetry restoration at finite temperature (or for a large number of quark flavors) connected with the formation of instanton–anti-instanton molecules.

CONTENTS

0163-8998/97/1201-0359$08.00

INTRODUCTION

Scales of Non-Perturbative QCD

Understanding the vacuum structure of strongly interacting gauge theories like quantum chromo-dynamics (QCD) is one of the most important problems in nuclear and particle physics today. Although QCD is now firmly established as the correct theory of the strong interactions, reliable calculations can only be performed in the perturbative domain (hard reactions with large momentum transfer). Studying non-perturbative aspects of QCD has proved to be a much more difficult task, in large part because the corresponding methods first had to be developed. There remains a large gap between QCD, where the main results come from hadronic phenomenology or numerical simulations on the lattice, and well-understood (or even exactly solvable) toy models, which are typically either 2-dimensional or supersymmetric. Although a number of fascinating discoveries have been made (instantons among them), much work remains to be done.

In order to develop a systematic strategy, it is important to establish whether the problem can be split into separate parts. As usual in physics, we expect this to be possible if a hierarchy of scales exists. In the case of QCD, there is some evidence that such a hierarchy is indeed available. One fundamental input comes from perturbative QCD. Although the value of the QCD scale parameter that enters perturbative calculations is $\Lambda_{\rm QCD} \sim 0.2\,{\rm GeV} \sim 1\,{\rm fm}^{-1}$ (the exact value depending on the definition), the applicability of the parton model to hard processes is limited to reactions involving a scale of at least 1 GeV.

Alternatively, an estimate of the scale of non-perturbative effects in QCD can be made on the basis of low-energy effective theories. The first estimate of the kind goes back to the Nambu & Jona-Lasinio (NJL) model (1). The model was developed in the early 1960s, inspired by the analogy between chiral symmetry breaking and superconductivity. It postulates a four-fermion interaction that, if it exceeds a certain strength, leads to quark condensation, the appearance of pions as Goldstone bosons, etc. The scale at which these interactions disappear and QCD becomes perturbative enters the model as an explicit UV cut-off, $\Lambda_{\chi{\rm SB}} \sim 1\,{\rm GeV}$.

In addition to that, one can argue that the scales for chiral symmetry breaking and confinement are very different (2): $\Lambda_{\chi{\rm SB}} \gg \Lambda_{\rm conf} \sim \Lambda_{\rm QCD}$. In particular,

it was proposed that constituent quarks (and pions) have sizes smaller than those of typical hadrons, explaining the success of the non-relativistic quark model. This idea was developed in a systematic fashion by Georgi & Manohar (3), who considered the ratio of these two scales as a natural expansion parameter in chiral effective Lagrangians. They also argued that an effective theory of pions and constituent quarks is the natural description in the intermediate regime $\Lambda_{\rm conf} < Q < \Lambda_{\chi \rm SB}$, in which models of hadronic structure operate.

Although the progress in understanding confinement is still very slow, the fundamental mechanism of chiral symmetry breaking has been clarified in significant detail. It is the purpose of this review to explain the main ideas and results. For a more detailed exposition and technical details, the reader is invited to consult the more comprehensive work (4). The picture of the vacuum that has emerged over the years has been termed the instanton liquid model (5). The main feature of this model is that the non-perturbative gluon fields are concentrated in well-localized ($\rho \sim 1/3$ fm) topological fluctuations, instantons, with very strong fields. The small size of the typical instanton is the reason why the parameter $\Lambda_{\chi \rm SB} \sim 1$ GeV is large, why the pion is small, why glueballs are heavy (6), etc.

In the remainder of this introduction we would like to give a brief discussion of hadronic structure from the perspective of the instanton liquid model and provide a short history of the subject. In Section 2, we discuss hadronic correlation functions and their importance in providing a bridge between hadronic phenomenology and the structure of the vacuum. In Sections 3 and 4, we introduce the instanton solution and discuss the vacuum structure of the instanton liquid, the mechanism for quark and gluon condensation as well as the effective interaction between quarks. In Section 5, we give a more detailed discussion of hadronic correlation functions and the hadronic spectrum. In Section 6, we discuss some issues related to the phase structure of QCD, in particular QCD at finite temperature, QCD with many flavors and supersymmetric generalizations of QCD. Section 7 finally provides a brief summary and outlook.

Hadronic Structure

Understanding the structure of hadrons and the regularities in the spectrum of hadrons is an old problem. Indeed, the first two attempts to understand hadronic structure, the non-relativistic quark model and current algebra, predate the development of QCD. The quark model provides a very simple and phenomenologically successful scheme to describe the spectrum and the properties of hadrons, based on the idea that hadrons are loosely bound composites of massive ($\sim$300 MeV) constituent quarks. On the other hand, current algebra led to the conclusion that the the current quark masses that appear as symmetry breaking terms in the Lagrangian are tiny, on the order of a few MeV.

To reconcile these seemingly conflicting results was one of the major challenges to model builders. Another important task is to understand the relative importance of the various forces acting between quarks. Hadronic models incorporate (*a*) perturbative one-gluon-exchange interactions, (*b*) confining (string) potentials, (*c*) pion or other collective exchanges and (*d*) quasi-local instanton-induced interactions (which can be either two- or three-body forces). To understand the interplay of these interactions on the basis of hadronic spectroscopy alone is probably impossible; below we argue that the systematic study of hadronic correlation functions is a much more appropriate tool.

Here, we only want to make a few comments on the role of these forces. First, from the study of hard processes and the analysis of correlation functions (determined from experiment or on the lattice), it has become clear that the perturbative treatment of gluon fields at the hadronic scale ($1\,\mathrm{fm} = (0.2\,\mathrm{GeV})^{-1}$) is impossible. Gluons propagate perturbatively only at distances $\ll 1\,\mathrm{GeV}^{-1}$.

Second, one may argue that the numerical role of confinement for the masses of hadrons made of light quarks appears to be small. It has been known for a long time that the effective confining potential that provides an optimal description of low-lying hadrons in the constituent quark model is weaker than the one deduced from heavy quark $\bar{c}c$, $\bar{b}b$ states. It is tempting to attribute this difference to the extended nature of constituent quarks, in contrast to the point-like *c* or *b* quark. Constituent quarks have form-factors and only interact with sufficiently soft gluonic modes. This can be simulated on the lattice by measuring the string tension after smoothing the gauge fields. An example is shown in Figure 1. Although the string tension (the slope at large distances) is the same for both potentials, the smoothed potential is much smaller for $r \leq 3a \sim 1\,\mathrm{fm}$. This suggests that the string potential only affects the tail of hadronic wave functions. This can be seen more explicitly by comparing hadronic correlators and wave functions in full and cooled[1] gauge configurations (8).

There is another indirect hint that confinement effects are not dominant in light hadrons. The MIT bag model (9) assumes that confinement leads to the creation of a bubble of the perturbative phase that contains valence quarks (and gluons) surrounded by the non-perturbative vacuum in which quarks are confined. Hadronic spectroscopy then determines the difference in vacuum energy between the two phases, the so-called bag pressure. It turns out that the MIT bag constant is more than an order of magnitude smaller than the phenomenologically determined non-perturbative energy density (10). This implies that non-perturbative vacuum fields like instantons are not completely expelled from the interior of hadrons, but only slightly modified.

[1]Cooling is a specific smoothing method designed to isolate instanton contributions.

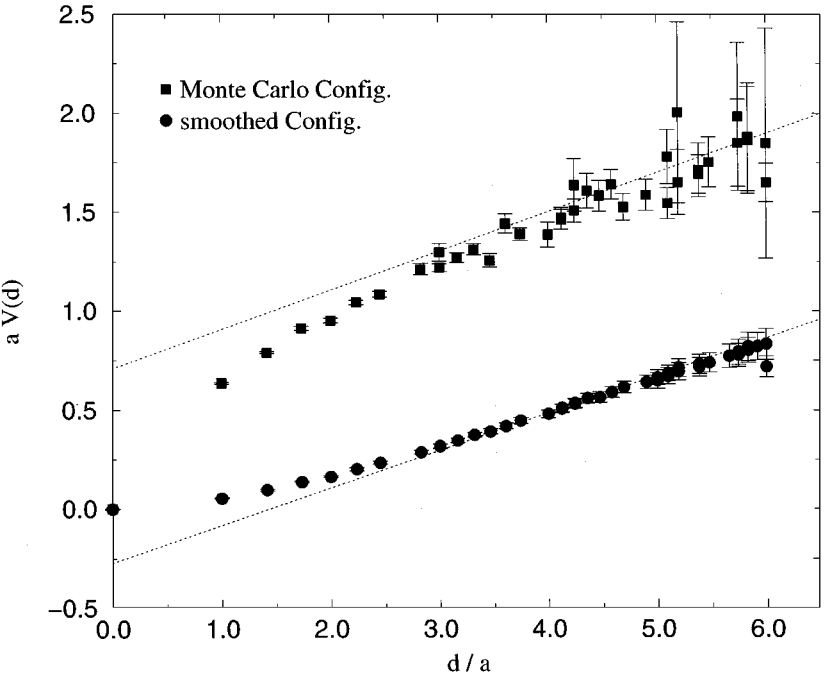

Figure 1 The $\bar{q}q$ potential before (above) and after (below) smoothing of the gauge fields, from Reference 7.

Over the years many hadronic models have been developed. These models cure many of the defects of the simple MIT bag model, particularly with regard to chiral symmetry. However, the relation between these models and the underlying field theory, QCD, remains unclear. This is hardly suprising; hadrons are collective excitations of the vacuum, like phonons in solids, so any model that attempts to reproduce their properties without addressing the structure of the ground state is meaningless.

Motivated by the hierarchy of scales discussed above, the strategy we wish to follow here is first to treat the phenomenon of chiral symmetry breaking. Starting from a satisfactory theory of constituent quarks and pions, one can go to the next scale and try to build a quantitative theory of hadrons. We will argue that the physics of chiral symmetry breaking is quite well understood, while the physical nature of confinement remains unclear. However, given the arguments above, this should provide a reasonable procedure for hadrons made of light quarks.

The importance of instantons in the context of chiral symmetry breaking is related to the fact that the Dirac operator has a chiral zero mode in the field of an

instanton. These zero modes correspond to localized quark states that can become collective if many instantons and anti-instantons interact. The resulting delocalized state corresponds to the wave function of the quark condensate. In addition to that, instanton zero modes generate an effective four-fermion interaction.

This brings us back to one of the oldest approaches to hadronic structure, the NJL model. Nambu & Jona-Lasinio showed that a short-range attractive force between fermions, if strong enough, can rearrange the vacuum, and the ground state becomes superconducting. There is a gap in the fermionic spectrum, corresponding to the constituent quark mass, and a non-zero quark condensate. The role of instantons in QCD (similar to that of phonon exchange in a superconductor) is to provide the fundamental mechanism for the four-fermion interaction. Instantons fix the strength of the interaction and its spin-isospin dependence. In addition to that, asymptotic freedom and the finite size of instantons provide a natural cutoff (as opposed to the ad hoc cutoff in the NJL model). Finally, a numerical but quite practical approach was developed, allowing calculations to all orders in the instanton-induced 't Hooft effective interaction.

A Brief Survey of Instanton Physics

In this section we would like to give a brief overview of instantons, their discovery, early applications and recent developments. Here, we mostly follow the historical path, while in Section 3 we will provide a more standard, systematic, discussion.

The instanton solution of the Yang-Mills equations was discovered by Polyakov and coworkers (11), motivated by the search for classical solutions that might be relevant for the large-distance behavior of Yang-Mills theories. Within a short time, a number of papers clarified the physical meaning of the instanton as a tunneling event between topologically distinct classical vacua (12–14). The tunneling rate was calculated in 't Hooft's classic paper (in which he also introduced the term instanton) (15), which also contains an important discovery: the presence of fermion zero modes in the spectrum of the Dirac operator. 't Hooft realized that these zero modes provide the microscopic mechanism for anomalies, the fact that quantum mechanically, the flavor singlet axial charge in QCD (or baryon number in electroweak theory) is not conserved.

In electroweak theory, the tunneling rate is suppressed by the vacuum expectation value of the Higgs field and therefore instanton effects are too small to be observable. In QCD, on the other hand, instanton effects are much larger, but the calculations are affected by infrared divergencies. Early attempts to study instantons effects in QCD were summarized in (16). This paper introduced the picture of the instanton ensemble as a 4-dimensional gas of pseudoparticles and

pointed out that instantons might be responsible for the spontaneous breakdown of $SU(N_f)$ chiral symmetry.

Nevertheless, they were not able to formulate a consistent theory of the instanton ensemble and the general outlook at that time was rather pessimistic: there was no clearly identified instanton effect, and no theoretical control over the semi-classical approximation in QCD. Eventually, a new impetus was provided when more phenomenological information on the structure of the QCD vacuum became available from the analysis of QCD sum rules (17). A particularly important conclusion was that the size of non-perturbative effects in scalar correlation functions, corresponding to the π, σ, η, η' mesons as well as scalar and pseudoscalar glueballs, is much bigger than in vector or tensor channels (18). It was realized that these are precisely those channels that receive direct instanton contributions (18–20). In addition to that, Witten and Veneziano suggested an approximate relation that connects the η' mass with the topological susceptibility (21, 22), providing the most direct estimate so far of the instanton density in QCD.

Based on these developments, the instanton liquid model was proposed by one of us (23). Its basic assumption is that instantons in QCD form a random liquid, characterized the mean density of instantons $n \simeq 1\,\mathrm{fm}^{-4}$ and their average size $\rho \sim 1/3\,\mathrm{fm}$. These parameters imply that the fraction of the space-time occupied by instantons $f \sim n\rho^4$ is small and that the semi-classical approximation is under control. They reproduce the values of the quark and gluon condensates, and the available information on the short-distance behavior of correlation functions.

Further steps towards providing a more sound theoretical basis for the instanton liquid model were taken in (24, 25). In addition to that, Diakonov and Petrov (26) introduced the picture of the quark condensate as a collective state built from delocalized zero modes and studied the properties of pseudoscalar meson in the random phase approximation (RPA). In parallel, one of us initiated numerical studies of the instanton liquid (27), which allows one to go beyond the mean field and RPA approximations. Finally, around that time, a number of authors began to study the properties of instantons directly on the lattice (see e.g. 28–31).

In the past few years, a lot of progress was made in the study of instantons in QCD. The instanton liquid model was used for large-scale, quantitative calculations of hadronic correlation functions in essentially all meson and baryon channels (32–34). Hadronic masses and coupling constants in most mesonic and baryonic channels were shown to be in quantitative agreement with phenomenology (35) and the lattice (36). It was shown how to go beyond the simple random instanton liquid and construct a self-consistent, interacting instanton ensemble (37, 38). The theory was also generalized to finite temperatures and

applied to the chiral phase transition. Some of these results will be reviewed in this paper.

In addition to that, a lot of effort went into studies of instantons on the lattice. Using a variety of methods such as cooling (39) or inverse blocking (40), one can produce a smoothed version of the original gauge field configuration and extract their classical content. Basically, these studies try to distill the instanton liquid from lattice configurations. The results are in very good agreement with the parameters of the instanton liquid model. The MIT group (8) also showed that cooling leaves the correlation functions of light hadrons essentially unaffected. This clearly suggests that the agreement between the lattice correlators and the results of the instanton model was not a coincidence. At the moment, very active work is going on in this direction, and in a few years we will understand the role of instantons in QCD on a much more quantitative level.

Finally, we would like to mention significant progress in understanding the role of instantons in supersymmetric extensions of QCD. Supersymmetric theories have the advantage that most higher-order perturbative effects cancel and instantons are the dominant non-perturbative effect left. An example is $N = 2$ supersymmetric gauge theory, for which the low-energy effective action was recently determined by Seiberg and Witten (41). The result can be expanded as a power series in the instanton density, and the coefficients can be checked against explicit instanton calculations (see 42–45). In addition to that, Seiberg and coworkers clarified the vacuum structure of the (more interesting) $N = 1$ supersymmetric extensions of QCD. Again, instantons play an important role. These results can potentially be generalized to non-supersymmetric theories and, maybe, ultimately to QCD.

CORRELATION FUNCTIONS AS A BRIDGE BETWEEN VACUUM AND HADRONIC STRUCTURE

In a (relativistic) field theory, correlation functions of gauge-invariant local operators are the proper tool to study the spectrum of the theory. The correlation functions can be calculated either from the physical states (mesons, baryons, glueballs) or in terms of the fundamental fields (quarks and gluons) of the theory. In the latter case, we have a variety of techniques at our disposal, ranging from perturbative QCD to the operator product expansion (OPE) to models of QCD and lattice simulations. For this reason, correlation functions provide a bridge between hadronic phenomenology on the one side and the underlying structure of the QCD vacuum on the other side.

Loosely speaking, hadronic correlation functions play the same role for understanding the forces between quarks as the NN scattering phase shifts did in the case of nuclear forces. In the case of quarks, however, confinement implies

that we cannot define scattering amplitudes in the usual way. Instead, one has to focus on the behavior of gauge invariant correlation functions at short and intermediate distance scales. The available theoretical and phenomenological information about these functions was recently reviewed in (35).

Euclidean point-to-point correlation functions are defined as

$$\Pi_h(x) = \langle 0|\, j_h(x)\, j_h(0)|0\rangle, \qquad 1.$$

where $j_h(x)$ is a local operator with the quantum numbers of a hadronic state h. We will concentrate on mesonic and baryonic currents of the type

$$j_{\rm mes}(x) = \delta^{ab}\bar{\psi}^a(x)\Gamma\psi^b(x), \qquad 2.$$

$$j_{\rm bar}(x) = \epsilon^{abc}(\psi^{a\,T}(x)C\Gamma\psi^b(x))\Gamma'\psi^c(x). \qquad 3.$$

Here, a, b, c are color indices and Γ, Γ' are isospin and Dirac matrices. In the following, we will only consider spacelike separations $\tau = \sqrt{-x^2}$. In this case, correlation functions are exponentially suppressed rather than oscillatory at large distance.

Hadronic correlation functions can be written in terms of the spectrum and the coupling constants of the physical excitations with the quantum numbers of the current j_h. This connection is based on the standard dispersion relation

$$\Pi(Q^2) = \frac{(-Q^2)^n}{\pi}\int \frac{{\rm Im}\Pi(s)}{s^n(Q^2+s)} + a_0 + a_1 Q^2 + \cdots, \qquad 4.$$

and the spectral decomposition ($\rho(s) \equiv \frac{1}{\pi}{\rm Im}\Pi(s)$)

$$\rho(s=-q^2) = (2\pi)^3 \sum_n \delta^4(q-q_n)\langle 0|\, j_h(0)|n\rangle\langle n|\, j_h^\dagger(0)|0\rangle. \qquad 5.$$

Here, $Q^2 = -q^2$ is the euclidean momentum transfer and we have indicated possible subtraction constants a_i. A spectral representation of the coordinate space correlation function is obtained by Fourier transforming Equation 4,

$$\Pi(\tau) = \int ds\, \rho(s) D(\sqrt{s}, \tau), \qquad 6.$$

where $D(m,\tau) = m/(4\pi^2\tau)K_1(m\tau)$ is the euclidean propagator of a scalar particle with mass m. Note that for large arguments the correlation function decays exponentially, $\Pi(\tau) \sim \exp(-m\tau)$, where the decay is governed by the lowest pole in the spectral function.

Correlation functions that involve quark fields only (like the meson and baryon currents introduced above) can be expressed in terms of the full quark

propagator. For an isovector meson current $j_{I=1} = \bar{u}\Gamma d$ (where Γ is only a Dirac matrix), the correlator only has a "one-loop" contribution

$$\Pi_{I=1}(x) = \langle \mathrm{Tr}\,[S^{ab}(0,x)\Gamma S^{ba}(x,0)\Gamma]\rangle. \qquad 7.$$

The averaging is performed over all gauge configurations, with the weight function $\det(\not{D} + m)\exp(-S)$. Correlators of isosinglet meson currents $j_{I=0} = \frac{1}{\sqrt{2}}(\bar{u}\Gamma u + \bar{d}\Gamma d)$ receive an additional two-loop, or disconnected, contribution

$$\Pi_{I=0}(\tau) = \langle \mathrm{Tr}\,[S^{ab}(0,x)\Gamma S^{ba}(x,0)\Gamma]\rangle - 2\langle \mathrm{Tr}\,[S^{aa}(0,0)\Gamma] \times \mathrm{Tr}\,[S^{bb}(x,x)\Gamma]\rangle. \qquad 8.$$

Analogously, baryon correlators can be expressed as vacuum averages of three quark propagators.

At short distance, asymptotic freedom implies that the correlation functions are determined by free quark propagation. Using the free quark propagator $S_0(x) \sim (\gamma \cdot x)/x^4$, we conclude that mesonic and baryonic correlation functions at short distance behave as $\Pi_{\mathrm{mes}} \sim 1/x^6$ and $\Pi_{\mathrm{bar}} \sim 1/x^9$, respectively. Deviations from asymptotic freedom at intermediate distances can be studied using the operator product expansion (OPE). The OPE systematically accounts for the interaction with non-perturbative quark and gluon condensates. Historically, QCD sum rules based on the OPE played an important role in establishing the connection between hadronic phenomenology and the structure of the QCD vacuum.

There are a number of sources for phenomenological information about hadronic correlation functions (35). The ideal situation is that the spectral function is determined from the optical theorem and an experimentally accessible cross section, as in the case of the vector-isovector (rho meson) channel from $\sigma(e^+e^- \to (I = 1\,\mathrm{hadrons}))$ and in the a_1 channel from hadronic decays of the τ lepton, $\Gamma(\tau \to \nu_\tau + \mathrm{hadrons})$. In most cases, the information is much more limited and only the contribution of a few resonances is known. The high-energy behavior, of course, can always be extracted from perturbation theory. Ultimately, the best source of information about hadronic correlation functions is the lattice. At present, most lattice calculations use complicated nonlocal sources, but some studies of correlation functions of local sources have been reported (36, 46).

Concluding this section, we would like to emphasize that any model of the QCD vacuum or of hadronic structure should be compared to the available information on hadronic correlation functions. Only in this way can the structure of hadrons and the effective forces between quarks be connected to the structure of the QCD vacuum.

INSTANTONS IN THE QCD VACUUM

Instantons and Tunneling

In this section we remind the reader of a few basic facts about instantons. All of this material can be found in reviews or textbooks (see for example 47, 48, 4). Instantons are solutions of the classical equations of motion in imaginary (or Euclidean) time. This means that, unlike solitons, instantons are not physical objects in Minkowski space but tunneling paths that connect different vacua of the theory.

Formally, instantons appear in the context of the semi-classical approximation to the (Euclidean) QCD partition function

$$Z = \int DA_\mu \, \exp(-S) \prod_f^{N_f} \det(\not{D} + m_f), \qquad 9.$$

$$S = \frac{1}{4g^2} \int d^4x \, G^a_{\mu\nu} G^a_{\mu\nu}. \qquad 10.$$

Here, S is the gauge field action and the determinant of the Dirac operator $\not{D} = \gamma_\mu(\partial_\mu - iA_\mu)$ accounts for the contribution of fermions. In the semi-classical approximation, we look for saddle points of the functional integral Equation 9, i.e. configurations that minimize the classical action S. This means that saddle point configurations are solutions of the classical equations of motion.

These solutions can be found using the identity

$$S = \frac{1}{4g^2} \int d^4x \left[\pm G^a_{\mu\nu} \tilde{G}^a_{\mu\nu} + \frac{1}{2} \left(G^a_{\mu\nu} \mp \tilde{G}^a_{\mu\nu} \right)^2 \right], \qquad 11.$$

where $\tilde{G}_{\mu\nu} = 1/2\epsilon_{\mu\nu\rho\sigma} G_{\rho\sigma}$ is the dual field strength tensor (the field strength tensor in which the roles of electric and magnetic fields are reversed). Since the first term is a topological invariant (see below) and the last term is always positive, it is clear that the action is minimal if the field is (anti) self-dual

$$G^a_{\mu\nu} = \pm \tilde{G}^a_{\mu\nu}. \qquad 12.$$

The action of a self-dual field configuration is determined by its topological charge

$$Q = \frac{1}{32\pi^2} \int d^4x \, G^a_{\mu\nu} \tilde{G}^a_{\mu\nu}. \qquad 13.$$

From Equation 11, we have $S = (8\pi^2|Q|)/g^2$. For finite action configurations, Q has to be an integer. The instanton is a solution with $Q = 1$ (11)

$$A^a_\mu(x) = \frac{2\eta_{a\mu\nu} x_\nu}{x^2 + \rho^2}, \qquad 14.$$

where the 't Hooft symbol $\eta_{a\mu\nu}$ is defined by

$$\eta_{a\mu\nu} = \begin{cases} \epsilon_{a\mu\nu} & \mu,\ \nu = 1,\ 2,\ 3, \\ \delta_{a\mu} & \nu = 4, \\ -\delta_{a\nu} & \mu = 4 \end{cases} \qquad 15.$$

and ρ is an arbitrary parameter characterizing the size of the instanton. The classical instanton solution has a number of degrees of freedom, known as collective coordinates. In addition to the size, the solution is characterized by the instanton position z_μ and the color orientation matrix R^{ab} (corresponding to color rotations $A^a_\mu \to R^{ab}A^b_\mu$). A solution with topological charge $Q = -1$ can be constructed by replacing $\eta_{a\mu\nu} \to \overline{\eta}_{a\mu\nu}$, where $\overline{\eta}_{a\mu\nu}$ is defined by changing the sign of the last two equations in Equation 15.

The physical meaning of the instanton solution becomes clear if we consider the classical Yang-Mills Hamiltonian (in the temporal gauge, $A_0 = 0$)

$$H = \frac{1}{2g^2}\int d^3x \left(E_i^2 + B_i^2\right), \qquad 16.$$

where E_i^2 is the kinetic and B_i^2 the potential energy term. The classical vacua corresponds to configurations with zero field strength. For non-abelian gauge fields this limits the gauge fields to be "pure gauge" $A_i = iU(\vec{x})\partial_i U(\vec{x})^\dagger$. Such configurations are characterized by a topological winding number n_W which distinguishes between gauge transformations U that are not continuously connected.

This means that there is an infinite set of classical vacua enumerated by an integer n. Instantons are tunneling solutions that connect the different vacua. They have potential energy $B^2 > 0$ and kinetic energy $E^2 < 0$, their sum being zero at any moment in time. Since the instanton action is finite, the barrier between the topological vacua can be penetrated, and the true vacuum is a linear combination $|\theta\rangle = \sum_n e^{in\theta}|n\rangle$ called the theta vacuum. In QCD, the value of θ is an external parameter. If $\theta \neq 0$ the QCD vacuum breaks CP invariance. Experimental limits on CP violation require[2] $\theta < 10^{-9}$.

The rate of tunneling between different topological vacua is determined by the semi-classical (WKB) method. From the single instanton action one expects

$$P_{\text{tunneling}} \sim \exp(-8\pi^2/g^2). \qquad 17.$$

The factor in front of the exponent can be determined by taking into account fluctuations $A_\mu = A^{cl}_\mu + \delta A_\mu$ around the classical instanton solution. This

[2]The question why θ happens to be so small is known as the "strong CP problem." Most likely, the resolution of the strong CP problem requires physics outside QCD and we will not discuss it any further.

calculation was performed in a classic paper by 't Hooft (15). The result is

$$dn_I = \frac{0.47\exp(-1.68N_c)}{(N_c-1)!(N_c-2)!}\left(\frac{8\pi^2}{g^2}\right)^{2N_c}\exp\left(-\frac{8\pi^2}{g^2(\rho)}\right)\frac{d^4z\,d\rho}{\rho^5}, \qquad 18.$$

where $g^2(\rho)$ is the running coupling constant at the scale of the instanton size. Taking into account quantum fluctuations, the effective action depends on the instanton size. This is a sign of the conformal (scale) anomaly in QCD. Using the one-loop beta function the result can be written as $dn_I/(d^4z) \sim d\rho\rho^{-5}(\rho\Lambda)^b$ where $b = (11N_c/3) = 11$ is the first coefficient of the beta function. Since b is a large number, small size instantons are strongly suppressed. On the other hand, there appears to be a divergence at large ρ. In this regime, however, the perturbative analysis based on the one-loop beta function is not applicable.

The Instanton Liquid

The discussion above concentrated on the effects of a single instanton, but in order to understand the structure of the QCD vacuum we have to consider ensembles with a finite density (N/V) of instantons and anti-instantons. Taking into account the interaction between instantons also provides us with a consistent method to deal with large size instantons. The instanton ensemble is described by the following partition function in the space of collective coordinates

$$Z = \sum_{N_+,\,N_-}\frac{1}{N_+!N_-!}\int\prod_i^{N_++N_-}[d\Omega_i\; n(\rho_i)]\exp(-S_{int})\cdot\prod_f^{N_f}\det(\not{D}+m_f), \qquad 19.$$

where $N_\pm$ is the number of (anti) instantons, $d\Omega_i = dU_i\, d^4z_i\, d\rho_i$ is the measure for the collective coordinates (color orientation, position and size) associated with individual instantons and $n(\rho)$ is the single instanton density given in Equation 18.

The partition function Equation 19 resembles a statistical mechanics system of four-dimensional pseudoparticles interacting via the bosonic interaction $S_{\rm int}$ and the (non-local) fermion determinant $\det(\not{D} + m_f)$. This means that we can evaluate the partition function using standard techniques from statistical mechanics, like the mean field approximation (MFA), variational methods or numerical Monte Carlo calculations. We will not go into detail here but refer the reader to the more extensive review (4). The simplest method is the mean field approximation. If we ignore all correlations among instantons, the partition function can be represented in terms of a single instanton distribution $\mu(\rho)$ (49)

$$Z \simeq \frac{1}{N_+!N_-!}\left(V\int d\rho\,\mu(\rho)\right)^{N_++N_-}. \qquad 20.$$

For small ρ, the instanton distribution is given by the single instanton result Equation 18 while for larger ρ interactions are important and the size distribution is modified. If the average effective interaction between instantons is repulsive, large instantons are suppressed and the distribution is peaked at some average size $\bar{\rho}$. Precisely how to define the interaction between very close (or very large) instantons is not very well understood. We will come back to this problem in the next section.

Let us mention a few simple predictions of the instanton liquid model. First, we would like to consider the gluon condensate. The volume integral of G^2 in the field of a single instanton is $32\pi^2$, independent of the size of the instanton. If we can ignore interactions between instantons, we get

$$\langle G^2 \rangle = (32\pi^2) \left(\frac{N}{V} \right). \qquad 21.$$

Due to tunneling, the energy density of the QCD vacuum is less than that of the perturbative vacuum (which we take to be zero). The classical energy density inside an instanton is zero everywhere (this is true for any self-dual field configuration), but quantum mechanically this result is modified. Consistency with the QCD trace anomaly requires that

$$\epsilon = -\frac{b}{4} \left(\frac{N}{V} \right), \qquad 22.$$

where b is the first coefficient of the beta function. This means that the energy density of the non-perturbative vacuum is about 1 GeV/fm^3 lower than the perturbative one.

Finally, let us consider the topological susceptibility, which is related to fluctuations of the topological charge. If the theta angle is zero, the average topological charge $\langle Q \rangle = \langle (N_+ - N_-) \rangle$ vanishes. In pure gauge theory, the instanton ensemble is fairly random and local fluctuations of the number of pseudoparticles are Poissonian. This means that $(N_+ - N_-) \sim \sqrt{N}$ and

$$\chi_{\rm top} = \lim_{V \to \infty} \frac{\langle Q^2 \rangle}{V} = \lim_{V \to \infty} \frac{\langle (N_+ - N_-)^2 \rangle}{V} \simeq \left(\frac{N}{V} \right). \qquad 23.$$

In the presence of light quarks, the situation is more complicated. Light quarks lead to correlations between instantons and anti-instantons and the topological charge is screened, $\chi_{\rm top} \simeq m \langle \bar{q} q \rangle$ and vanishes in the chiral limit. This result has important consequences for the properties of the η' meson.

Phenomenology of the Instanton Liquid

In order to determine the total tunneling rate in QCD from the standard semiclassical theory, one has to face the problem connected with large size instantons. We have seen that one way to solve this problem is to have a repulsive

effective interaction between instantons. However, in the relevant regime the interaction is not very well defined.[3]

In this section, we want to give a review of the available information on the instanton distribution in QCD, coming from both hadronic phenomenology and the lattice. The first attempt of this type was made by Shifman et al in (50). These authors used the value of the gluon condensate $\langle 0|(G^a_{\mu\nu})^2|0\rangle \simeq 0.5\,\mathrm{GeV}^4$ obtained from a QCD sum rule analysis of the charmonium spectrum (17). If the gluon condensate is dominated by (weakly interacting) instantons, then we can estimate their density from Equation 21. This estimate provides an *upper limit* for the instanton density

$$\left(\frac{N}{V}\right) \leq \frac{1}{32\pi^2}\left\langle \left(G^a_{\mu\nu}\right)^2\right\rangle \simeq 1\,\mathrm{fm}^{-4}. \qquad 24.$$

A similar estimate can be obtained from the (pure gauge) topological susceptibility. The value of χ_{top} in quenched QCD can be estimated from the Witten-Veneziano relation (51, 22)

$$\chi_{\mathrm{top}} = 2f_\pi^2\left(m_\eta^2 + m_{\eta'}^2 - 2m_K^2\right) = (180\ \mathrm{MeV})^4. \qquad 25.$$

Using Equation 23, we again get $(N/V) \simeq 1\,\mathrm{fm}^{-4}$.

The other important parameter characterizing the instanton ensemble is the typical instanton size. If the total tunneling rate can be calculated from the semi-classical 't Hooft formula, then we can estimate the critical size by determining the maximum size up to which the rate has to be integrated in order to reproduce the phenomenological instanton density

$$\int_0^{\rho_{\max}} d\rho\, n_{\mathrm{scl}}(\rho) = n_{\mathrm{phen}}. \qquad 26.$$

Using $n_{\mathrm{phen}} = 1\,\mathrm{fm}^{-4}$, Shifman et al concluded that $\rho_{\max} \simeq 1\,\mathrm{fm}$. This is a very pessimistic result, because it implies that there are no individual instantons and that their action is not large, so the semi-classical approximation is useless.

However, if instantons interact, the situation may be different. The role of interactions can also be estimated using the value of the gluon condensate

$$dn = dn_{\mathrm{scl}}\left[1 + \frac{\pi^4\rho^4}{2g^4}\left\langle \left(G^a_{\mu\nu}\right)^2\right\rangle + \cdots\right]. \qquad 27.$$

Using the canonical value of the gluon condensate, we see that for $\rho > 0.2$ fm the interaction of instantons with the gluon condensate cannot be neglected. Also, we observe that interactions lead to a tunneling rate that grows faster than

[3]A more extensive discussion of the current status of this problem can be found in (4).

the semi-classical rate. Based on this result, one of us (23) suggested that the typical instanton size is significantly smaller,

$$\rho_{\max} \sim 1/3\,\text{fm}. \tag{28.}$$

If the average instanton is indeed small, we obtain a completely different picture of the QCD vacuum:

1. Since the instanton size is significantly smaller than the typical separation R between instantons, $\rho/R \sim 1/3$, the vacuum is fairly dilute. The fraction of spacetime occupied by strong fields is only a few percent.

2. The fields inside the instanton are very strong $G_{\mu\nu} \gg \Lambda^2$. This means that the semi-classical approximation is valid, and the typical action is large

$$S_0 = 8\pi^2/g^2(\rho) \sim 10 - 15 \gg 1. \tag{29.}$$

   Higher-order corrections are proportional to $1/S_0$ and presumably small.

3. Instantons retain their individuality and are not destroyed by interactions. From the dipole formula, one can estimate

$$|\delta S_{\text{int}}| \sim (2-3) \ll S_0. \tag{30.}$$

4. Nevertheless, interactions are important for the structure of the instanton ensemble, since

$$\exp|\delta S_{\text{int}}| \sim 20 \gg 1. \tag{31.}$$

   This implies that interactions have a significant effect on correlations among instantons; the instanton ensemble in QCD is not a dilute gas but an interacting liquid.

Improved estimates of the instanton size can be obtained from phenomenological applications of instantons. The average instanton size determines the structure of chiral symmetry breaking, in particular the values of the quark condensate, the pion mass, its decay constant and form factor. We will discuss these observables in more detail below.

The most direct way to determine properties of the instanton liquid is provided by numerical simulations on the lattice. In these simulations one can identify individual instantons and study their distribution. In practice, this is a very technical subject and we will not go into much detail here. The simplest method of this type is the cooling algorithm, which is based on locally minimizing the action in order to extract the semi-classical content of a given gauge

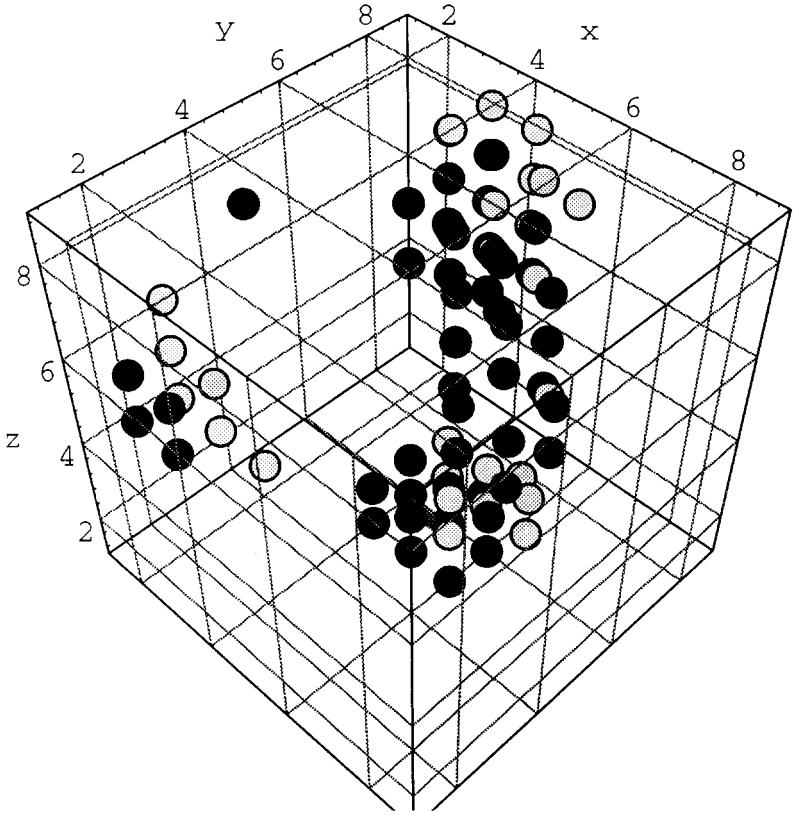

Figure 2 Cooled lattice configuration (on a Euclidean time slice) in $SU(3)$ gauge theory with dynamical quarks, from (52). The dark dots represent the topological charge distribution and the light dots the chiral condensate.

configuration.[4] After the quantum noise disappears, one can identify classical objects and determine their properties. As an example, Figure 2 shows the topological charge distribution in a cooled lattice configuration (52). Also plotted is the distribution of the quark condensate, showing that there is a strong correlation of the condensate with instantons. From an analysis of many configurations of this type, the MIT group of Chu et al concludes that the instanton density in pure gauge QCD is $(1.3-1.6)\ \mathrm{fm}^{-4}$ (8). This number is indeed quite close to the estimates presented above.

[4]There are several problems with this method. For example, instantons and anti-instantons tend to annihilate during the cooling procedure.

The average instanton size can be obtained by fitting the topological charge correlation function after cooling. The fit is very good and gives an average size $\rho = 0.35\,\text{fm}$ (8). More detail is provided by measurements of the instanton size distribution. Recently the first lattice study of this type was performed for purge gauge $SU(2)$ (53). The result qualitatively agrees with the semi-classical prediction for small radii (although for small ρ, distortions due to the finite lattice size are important), but shows a strong suppression of large-size instantons. As emphasized above, the physical mechanism for this effect is not adequately understood. The lattice result can be described either in terms of a repulsive core in the instanton interaction, or by non-perturbative modifications of the beta function that enters the single instanton distribution (54).

INSTANTONS AND LIGHT QUARKS

Zero Modes and the $U(1)_A$ Anomaly

In the last section we showed that instantons interpolate between different topological vacua in QCD. It is then natural to ask if the different vacua can be physically distinguished. This question is answered most easily in the presence of light fermions, because the different vacua have different axial charge. This observation is the key element in understanding the mechanism of chiral anomalies.

Anomalies first appeared in the context of perturbation theory (55, 56). From the axial vector–two gluon (AW) triangle diagram current one finds that the flavor singlet current which is conserved on the classical level develops an anomalous divergence on the quantum level

$$\partial_\mu j^5_\mu = \frac{N_f}{16\pi^2} G^a_{\mu\nu} \tilde{G}^a_{\mu\nu}. \qquad 32.$$

This anomaly plays an important role in QCD, because it explains the absence of a ninth Goldstone boson, the so-called $U(1)_A$ puzzle.

The mechanism of the anomaly is intimately connected with instantons. First, we recognize the integral of the RHS of Equation 32 as $2N_f Q$, where Q is the topological charge. This means that in the background field of an instanton we expect axial charge conservation to be violated by $2N_f$ units. The crucial property of instantons, originally discovered by 't Hooft, is that the Dirac operator has a zero mode $i\not{D}\psi_0(x) = 0$ in the instanton field. For an instanton in the singular gauge, the zero mode wave function is

$$\psi_0(x) = \frac{\rho}{\pi} \frac{1}{(x^2+\rho^2)^{3/2}} \frac{\gamma \cdot x}{\sqrt{x^2}} \frac{1+\gamma_5}{2} \phi, \qquad 33.$$

where $\phi^{\alpha m} = \epsilon^{\alpha m}/\sqrt{2}$ is a constant spinor, which couples the color index α to

the spin index $m = 1, 2$. Note that the solution is left-handed, $\gamma_5\psi_0 = -\psi_0$. Analogously, in the field of an anti-instanton there is a right-handed zero mode.

We can now see how axial charge conservation is violated during tunneling (57, 58). For this purpose, let us consider the Dirac Hamiltonian $i\vec{\alpha}\cdot\vec{D}$ in the field of the instanton. The presence of a 4-dimensional normalizable zero mode implies that there is one left-handed state that crosses from positive to negative energy during the tunneling event. This can be seen as follows: In the adiabatic approximation, solutions of the Dirac equation are given by

$$\psi_i(\vec{x}, t) = \psi_i(\vec{x}, t = -\infty) \exp\left(-\int_{-\infty}^{t} dt' \epsilon_i(t')\right). \qquad 34.$$

The only way we can have a 4-dimensional normalizable wave function is if ϵ_i is positive for $t \to \infty$ and negative for $t \to -\infty$. This explains how axial charge can be changed during tunneling. No fermion ever changes its chirality; all states simply move one level up or down. The axial charge comes, so to say, from the "bottom of the Dirac sea."

The Effective Interaction Between Quarks

Proceeding from pure glue theory to QCD with light quarks, one has to deal with the much more complicated problem of quark-induced interactions. Indeed, on the level of a single instanton we cannot even understand the presence of instantons in full QCD. The reason is again related to the existence of zero modes. In the presence of light quarks, the tunneling rate is proportional to the fermion determinant, which is given by the product of the eigenvalues of the Dirac operator. This means that (as $m \to 0$) the tunneling amplitude vanishes and individual instantons cannot exist!

This result is related to the anomaly: During the tunneling event, the axial charge of the vacuum changes, so instantons have to be accompanied by fermions. The tunneling amplitude is non-zero only in the presence of external quark sources, because zero modes in the denominator of the quark propagator can cancel against zero modes in the determinant. Consider the fermion propagator in the instanton field

$$S(x, y) = \frac{\psi_0(x)\psi_0^+(y)}{im} + \sum_{\lambda\neq 0} \frac{\psi_\lambda(x)\psi_\lambda^+(y)}{\lambda + im}, \qquad 35.$$

where $i\not{D}\psi_\lambda = \lambda\psi_\lambda$. For N_f light quark flavors the instanton amplitude is proportional to m^{N_f}. Instead of the tunneling amplitude, let us calculate a $2N_f$-quark Green's function $\langle\prod_f \bar{\psi}_f(x_f)\Gamma\psi_f(y_f)\rangle$, containing one quark and antiquark of each flavor. Performing the contractions, the amplitude involves N_f fermion propagators Equation 35, so that the zero mode contribution involves a factor m^{N_f} in the denominator.

The result can be written in terms of an effective Lagrangian (15). It is a non-local $2N_f$-fermion interaction, where the quarks are emitted or absorbed in zero mode wavefunctions. The result simplifies if we take the long wavelength limit (in reality, the interaction is cut off at momenta $k > \rho^{-1}$) and average over the instanton position and color orientation. For $N_f = 1$ the result is (59, 60)

$$\mathcal{L}_{N_f=1} = \int d\rho\, n_0(\rho) \left(m\rho - \frac{4}{3}\pi^2\rho^3 \bar{q}_R q_L \right), \qquad 36.$$

where $n_0(\rho)$ is the tunneling rate. Note that the zero mode contribution acts like a mass term. For $N_f = 1$, there is only one chiral $U(1)$ symmetry, which is anomalous. This means that the anomaly breaks chiral symmetry and gives a fermion mass term. This is not true for more than one flavor. For $N_f = 2$, the result is

$$\mathcal{L}_{N_f=2} = \int d\rho\, n_0(\rho) \left[\prod_f \left(m\rho - \frac{4}{3}\pi^2\rho^3 \bar{q}_{f,R} q_{f,L} \right) + \frac{3}{32} \left(\frac{4}{3}\pi^2\rho^3 \right)^2 \times \left(\bar{u}_R \lambda^a u_L \bar{d}_R \lambda^a d_L - \bar{u}_R \sigma_{\mu\nu} \lambda^a u_L \bar{d}_R \sigma_{\mu\nu} \lambda^a d_L \right) \right]. \qquad 37.$$

One can easily check that the interaction is $SU(2) \times SU(2)$ invariant, but $U(1)_A$ is explicitly broken. This Lagrangian is of the type first studied by Nambu and Jona-Lasinio (1) and widely used as a model for chiral symmetry breaking and as an effective description for low-energy chiral dynamics (61, 62, 63).

Unlike the NJL model, however, the instanton-induced interaction has a natural cut-off parameter ρ, and the coupling constants are not free parameters, but determined by a physical quantity, the instanton density. The interaction is attractive for quark-antiquark pairs with the quantum numbers of the π and σ meson. If the interaction is sufficiently strong, it can rearrange the vacuum and lead to quark condensation and a light (Goldstone) pion. We will study these phenomena in much more detail below.

The Quark Condensate in the Mean Field Approximation

We showed in the last section that in the presence of light fermions, tunneling can only take place if the tunneling event is accompanied by N_f fermions which change their chirality. But in the QCD vacuum, chiral symmetry is broken and the quark condensate $\langle \bar{q}q \rangle = \langle \bar{q}_L q_R + \bar{q}_R q_L \rangle$ is non-zero. This means that there is a finite amplitude for a quark to change its chirality and we expect the instanton density to be finite.

For a sufficiently dilute system of instantons, we can estimate the instanton density in full QCD from the expectation value of the $2N_f$ fermion operator in the effective Lagrangian Equation 37. Using the factorization assumption (17),

we find that the factor $\prod_f m_f$ in the instanton density should be replaced by $\prod_f m_f^*$, where the effective quark mass is given by

$$m_f^* = m_f - \frac{2}{3}\pi^2\rho^2\langle\bar{q}_f q_f\rangle. \quad 38.$$

This shows that if chiral symmetry is broken, the instanton density is finite in the chiral limit.

This obviously raises the question whether the quark condensate itself can be generated by instantons. This question can be addressed using several different techniques (for a review, see 4, 64). One possibility is to use the effective interaction Equation 37 and to calculate the quark condensate in the mean field (Hartree-Fock) approximation. This corresponds to summing the contribution of all "cactus" diagrams to the full quark propagator. The result is a gap equation (26)

$$\int \frac{d^4k}{(2\pi)^4}\frac{M^2(k)}{k^2+M^2(k)} = \frac{N}{4N_cV}, \quad 39.$$

which determines the constituent quark mass $M(0)$ in terms of the instanton density (N/V). Here, $M(k) = M(0)k^2\varphi'^2(k)/(2\pi\rho)$ is the momentum dependent effective quark mass and $\varphi'(k)$ is the Fourier transform of the zero mode profile Equation 26. The quark condensate is given by

$$\langle\bar{q}q\rangle = -4N_c\int\frac{d^4k}{(2\pi)^4}\frac{M(k)}{M^2(k)+k^2}. \quad 40.$$

Using our standard parameters $(N/V) = 1\,\text{fm}^{-4}$ and $\rho = 1/3$ fm, one finds $\langle\bar{q}q\rangle \simeq -(255\ \text{MeV})^3$ and $M(0) = 320$ MeV. Parametrically, $\langle\bar{q}q\rangle \sim (N/V)^{1/2}\rho^{-1}$ and $M(0) \sim (N/V)^{1/2}\rho$. Note that both quantities are proportional not to (N/V), but to $(N/V)^{1/2}$. This is a reflection of the fact that spontaneous breaking of chiral symmetry is not a single instanton effect, but involves infinitely many instantons.

A very instructive way to study the mechanism for chiral symmetry breaking at a more microscopic level is by considering the distribution of eigenvalues of the Dirac operator. A general relation that connects the spectral density $\rho(\lambda)$ of the Dirac operator to the quark condensate was given by Banks and Casher (65),

$$\langle\bar{q}q\rangle = -\pi\rho(0). \quad 41.$$

This result is analogous to the Kondo formula for the electrical conductivity. Just like the conductivity is given by the density of states at the Fermi surface, the quark condensate is determined by the level density at zero virtuality λ. For a disordered, random, system of instantons the zero modes interact and form

a band around $\lambda = 0$. As a result, the eigenstates are delocalized and chiral symmetry is broken. On the other hand, if instantons are strongly correlated, for example bound into topologically neutral molecules, the eigenvalues are pushed away from zero, the eigenstates are localized and chiral symmetry is unbroken. As we will see in Section 6, precisely which scenario is realized depends on the parameters of the theory, like the number of light flavors and the temperature. Of course, for "real" QCD with two light flavors at $T = 0$, we expect chiral symmetry to be broken. This is supported by numerical simulations of the partition function of the instanton liquid (38).

HADRONS AND CORRELATORS

Quark Propagation in the Instanton Liquid

In Section 2 we saw that hadronic correlation functions are the basic tool to study hadronic spectroscopy. We also emphasized that hadronic correlators are determined by ensemble averages of traces involving the fermion propagator. For this reason, we want to start by studying the propagation of quarks in the instanton liquid in a little more detail.

The quark propagator is defined by $S(x, y) = \langle x|(i\not{D} + im)^{-1}|y\rangle$. In the instanton liquid, a distinguished role is played by the zero modes of the individual instantons. We therefore write the propagator as

$$S(x, y) = \sum_{IJ} \psi_I(x) \left(\frac{1}{T + im} \right)_{IJ} \psi_J^\dagger(y) + S_{\text{nzm}}(x, y), \qquad 42.$$

where ψ_I is the zero mode wave function associated with the Ith instanton, $T_{IJ} = \langle \psi_I | i\not{D} | \psi_J \rangle$ is a matrix element of the Dirac operator and S_{nzm} denotes the non-zero mode part of the quark propagator. The propagator Equation 42 has a simple interpretation: quarks propagate in the instanton liquid by jumping from one instanton zero mode to the other. The amplitude for this process is controlled by the hopping matrix elements T_{IJ}.

In the vicinity of a given instanton, the propagator is dominated by the contribution of the closest instanton $I = I_*$

$$S(x, y) \simeq \psi_{I_*}(x) \left(\frac{1}{T + im} \right)_{I_* I_*} \psi_{I_*}^\dagger(y) \simeq \frac{\psi_{I_*}(x) \psi_{I_*}^\dagger(y)}{m^*}. \qquad 43.$$

As a result, the propagator looks like the propagator Equation 35 in the field of a single instanton, but with the current mass replaced by an effective mass $(m^*)^{-1} = N^{-1} \sum (\lambda + im)^{-1}$. In the mean field approximation, we have $m^* = \pi\rho(2n/3)^{1/2}$.

The propagator Equation 43 can be used to estimate the effects of single instantons on hadronic correlation functions. The effect of interactions is only

represented by the effective mass m^*, which takes into account that chiral symmetry is broken. As an example, let us consider the pion correlation function. In the single instanton approximation, we have (20)

$$\Pi_\pi^{\mathrm{SIA}}(x) = \int d\rho\, n(\rho) \frac{6\rho^4}{\pi^2} \frac{1}{(m^*)^2} \frac{\partial^2}{\partial (x^2)^2} \left\{ \frac{4\xi^2}{x^4} \left(\frac{\xi^2}{1-\xi^2} + \frac{\xi}{2} \log \frac{1+\xi}{1-\xi} \right) \right\}, \quad 44.$$

where $\xi^2 = x^2/(x^2 + 4\rho^2)$. The result is shown in Figure 3, normalized to

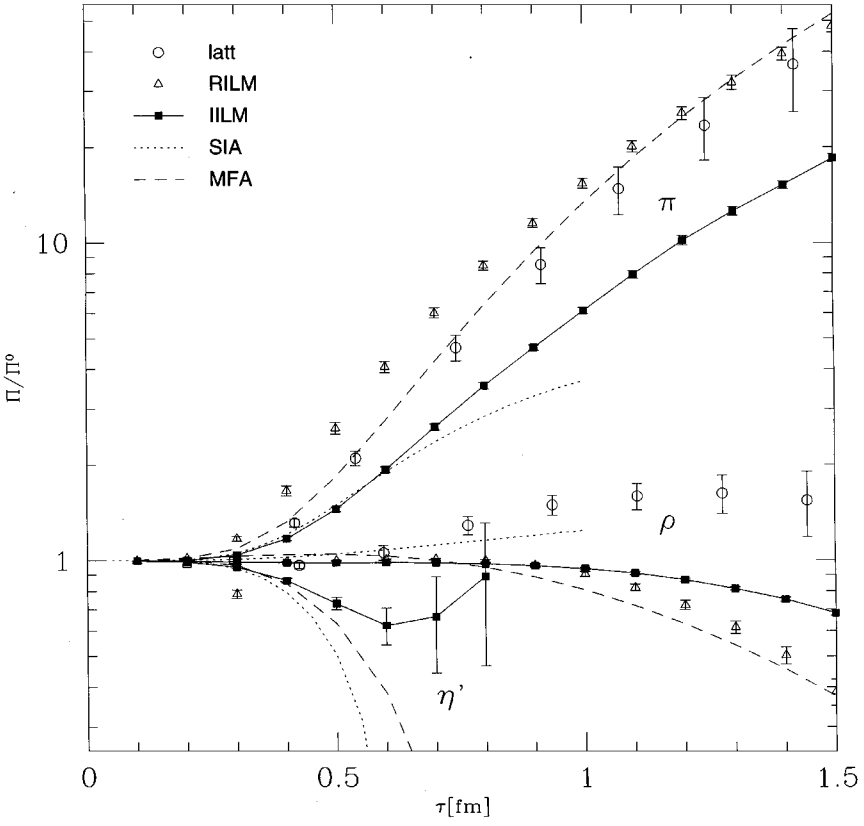

Figure 3 Pion, rho meson and eta prime correlation functions. All correlators are normalized to their perturbative behavior. We show the results in the random (RILM) and interacting instanton liquid (IILM), the single instanton approximation (SIA) and the random phase approximation (MFA), compared to quenched lattice results reported in (46).

the perturbative contribution. Clearly, instantons provide a strongly attractive interaction in the pion channel. If we repeat this simple exercise in other meson channels, we find that the same attraction also operates in the scalar σ channel, but that the interaction in the η' and the scalar-isovector δ channel is repulsive. Also, on this level there is no instanton contribution to the vector meson channels ρ, a_1, ω, b_1.

The single-instanton contribution correctly describes the correlation functions at intermediate distances $x \simeq (0.2-0.5)$ fm. However, in order to understand the large distance behavior and accommodate the formation of hadronic bound states, we have to sum up the effects of the single instanton ('t Hooft) interaction. In the next section we will present numerical results in which this has been accomplished by inverting the Dirac operator in the zero mode zone. Before we get to this, we would like to discuss a simpler method where the effective interaction (37) is treated in the random phase approximation (RPA). This amounts to summing all "fish" diagrams in the correlation function. The result can be written as $\Pi^{\rm RPA}(x) = \Pi^{\rm MFA}(x) + \Pi^{\rm int}$ (26, 66, 67), where $\Pi^{\rm MFA}$ denotes the mean field contribution and

$$\Pi^{\rm int}_{\pi,\eta'}(x) = \int d^4q\, e^{iq\cdot x}\Gamma_5(q)\frac{\pm 1}{1\mp C_5(q)}\Gamma_5(q). \qquad 45.$$

Here, C_5 denotes the elementary loop function and Γ_5 the vertex function

$$C_5(q) = 4N_c\left(\frac{V}{N}\right)\int\frac{d^4p}{(2\pi)^4}\frac{M_1M_2\big(M_1M_2 - p_1\cdot p_2\big)}{\big(M_1^2+p_1^2\big)\big(M_2^2+p_2^2\big)}, \qquad 46.$$

$$\Gamma_5(q) = 4\int\frac{d^4p}{(2\pi)^4}\frac{\sqrt{M_1M_2}\big(M_1M_2 - p_1\cdot p_2\big)}{\big(m_1^2+p_1^2\big)\big(M_2^2+p_2^2\big)}, \qquad 47.$$

with $p_1 = p + q/2$, $p_2 = p - q/2$ and $M_{1,2} = M(p_{1,2})$. Equation 45 has the typical form of an RPA correlator which arises from summing a geometric progression of elementary bubbles. The pion channel is very attractive and has a pole if $1 - C_5(q) = 0$. It is easy to check that for massless current quarks this condition is satisfied for $q^2 = 0$, corresponding to a massless pion. The pion decay constant is given by

$$f_\pi^2 = 4N_c\int\frac{d^4p}{(2\pi)^4}\frac{M^2(p)}{(p^2+M^2(p))^2} \simeq (100\ \text{MeV})^2, \qquad 48.$$

in good agreement with experiment. Parametrically, $f_\pi \sim \rho(N/V)^{1/2} \sim \rho^{-1}(\rho^4 N/V)^{1/2}$, so f_π is small because the instanton liquid is dilute, $(\rho^4 N/V)^{1/2} \simeq 1/10$.

Light Hadrons in the Instanton Liquid

In order to go beyond the mean field approximation and to study channels that do not receive first-order instanton contributions, it is desirable to calculate the correlation functions to all orders in the 't Hooft interaction. This can be achieved by performing numerical calculations in the interacting instanton liquid (32, 33, 34). These calculations are done in two steps.

First, we have to construct the appropriate instanton ensemble. This is accomplished by performing Monte Carlo simulations of the partition function (19). We have considered correlation functions in three different ensembles, the random ensemble (RILM), the quenched (QILM) and fully interacting (IILM) instanton ensembles. In the random model, we completely ignore the interaction between instantons and all collective coordinates are distributed randomly (except for the size, which is kept fixed). In the quenched approximation, the ensemble takes into account correlations due to the bosonic interaction, while the fully interacting ensemble also includes correlations induced by the fermion determinant. In both cases, the instanton density and size distribution are determined self-consistently.

The second step is the calculation of the fermion propagator and the hadronic correlation functions in a given ensemble. The propagator is constructed based on Equation 42, using the analytically known zero mode wave functions and overlap matrix elements, as well as the non-zero mode propagator in the field of a single instanton. The correlation functions are traces $\mathrm{tr}[S(\tau)\Gamma S(-\tau)\Gamma]$ and $\mathrm{tr}[S(\tau)\Gamma S(\tau)\Gamma S(\tau)\Gamma]$ for mesons and baryons, respectively, averaged over the instanton ensemble. Note that the averaging automatically includes the interaction to all orders, not just the one-loop graph. Finally, we determine the mass and the coupling constant of the lowest resonance by fitting the correlation function with the spectral representation Equation 6, using a simple model for the spectral function.

As an example we show the results in the π, ρ, η' meson and N, Δ baryon channels in Figures 3 and 4. In the pion channel, the interaction is very attractive, as one can see from the single instanton approximation (SIA). For distances $x > 0.5$ fm, the single instanton vertex has to be resummed in order to reproduce the full correlation function. The RPA correlator is somewhat larger than the correlator in the fully interacting ensemble, but the difference is essentially due to different values of the quark condensate (and the fact that, for technical reasons, the interacting correlator is calculated for a fairly large current quark mass). Both correlation functions correspond to the right value of the pion mass.[5] In Figures 3 and 4, we also show quenched lattice results reported in

[5]In the case of the interacting ensemble, the pion mass has to be extrapolated to physical values of the current quark mass.

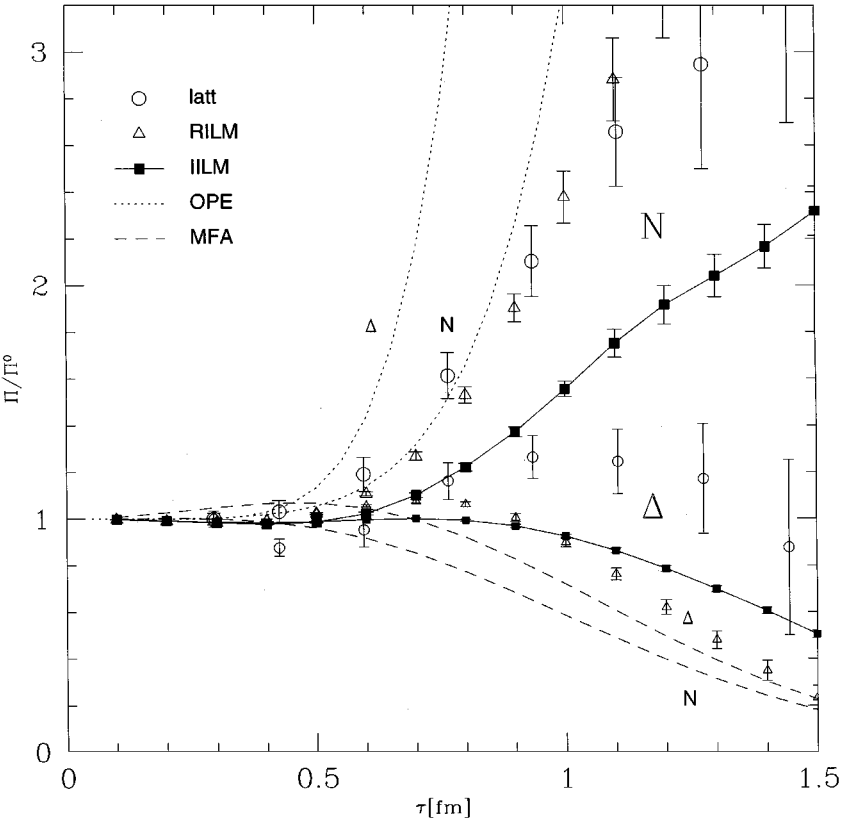

Figure 4 Nucleon and delta correlation functions. All correlators are normalized to their perturbative behavior. We show the results in the random (RILM) and interacting instanton liquid (IILM), the operator product expansion (OPE) and the mean field approximation (MFA), compared to quenched lattice results reported in (46).

(46). These results should be compared with the quenched (QILM) instanton model predictions, and indeed the agreement is quite good.

In the case of the η', both the single-instanton approximation and the RPA are too repulsive. This is one of the few channels where the quenched approximation leads to completely wrong results and correlations induced by the fermion determinant are crucial in order reproduce experiment. In the quenched approximation, the correlation function becomes unphysical for $x > 0.5$ fm. In the full ensemble, topological charge screening leads to the formation of

Table 1 Meson parameters in the different instanton ensembles. All quantities are given in units of GeV. For technical reasons the current quark mass is $m_u = m_d \simeq 20\,MeV$. Except for the pion mass, no attempt has been made to extrapolate the parameters to physical values of the quark mass

	Unquenched	Quenched	RILM
m_π	0.265	0.268	0.284
m_π (extr.)	0.117	0.126	0.155
λ_π	0.214	0.268	0.369
f_π	0.071	0.091	0.091
m_ρ	0.795	0.951	1.000
g_ρ	6.491	6.006	6.130
m_{a_1}	1.265	1.479	1.353
g_{a_1}	7.582	6.908	7.816
m_σ	0.579	0.631	0.865
m_δ	2.049	3.353	4.032
$m_{\eta_{\rm ns}}$	1.570	3.195	3.683

instanton–anti-instanton pairs, which provide an attractive interaction that balances some of the repulsion.

In the rho-meson channel the correlation function is close to the free correlator for all distances up to $x \simeq 1.5$ fm. Note that there is no first order instanton-induced interaction, so the mean field approximation corresponds to non-interacting constituent quarks. Taking the interaction into account to all orders, there is some binding in the ρ meson channel. In the full ensemble, we find $m_\rho = 795$ MeV, in good agreement with the experimental value $m_\rho = 770$ MeV. A more detailed comparison of the results in different instanton ensembles can be found in Table 1.

The chiral-even component of the nucleon and delta correlation functions is shown in Figure 4 [see (33) for a definition of the independent correlation functions]. The most important point is that the nucleon correlation function is much more attractive than the delta correlator. This is not captured by the OPE or the mean field approximation but is in agreement with lattice results (36). The nucleon mass is $m_N = 1.019$ GeV, in good agreement with experiment,[6] while the delta resonance is somewhat too heavy (see Table 2).

There are many more correlation functions that have been studied in the instanton liquid (see 4 and the original literature). In addition to hadrons made of light quarks, a number of authors have studied heavy-light (5, 32, 68) and

[6]Again, the current-quark mass is heavier than the physical value.

Table 2 Baryon parameters in different instanton ensembles. All quantities are given in units of GeV. The current quark mass is $m_u = m_d \simeq 20\,\text{MeV}$, larger than the physical value

	Unquenched	Quenched	RILM
m_N	1.019	1.013	1.040
λ_N^1	0.026	0.029	0.037
λ_N^2	0.061	0.074	0.093
m_Δ	1.428	1.628	1.584
λ_Δ	0.027	0.040	0.036

heavy quark systems (69) as well as glueballs (6). The instanton model reaches its limitations when one goes to systems that are dominated by the Coulomb interaction or confinement forces, such as heavy quark systems. We have argued that instantons play an important role in scalar glueball channels (6). Instantons are localized regions with a very large field strength that correspond to a strong attractive interaction in the scalar 0^{++} glueball channel and a very repulsive force in the pseudoscalar 0^{-+} channel. This is compatible with the fact that the scalar is the lightest glueball while the pseudoscalar is significantly heavier, and with lattice measurements that indicate a very compact wave function for the scalar glueball (70).

THE PHASES OF QCD

In this section we want to give a brief discussion of current ideas concerning the phase structure of QCD and QCD-like theories. This includes QCD at high temperature, non-abelian gauge theory for different numbers of colors N_c and flavors N_f, and supersymmetric extensions of QCD which include additional fields such as gluinos (fermions in the same color representation as the gluon) and scalar partners of quarks (squarks). The reader should be warned that, unlike the material above, which is based on a lot of data analysis and detailed lattice studies, many of these ideas are not yet firmly established and are currently under intense discussion.

Heating the Vacuum

At sufficiently high temperature (and/or density) QCD is predicted to undergo a phase transition to a new state (referred to as the quark-gluon plasma, QGP) in which chiral symmetry is restored and color changes are screened rather than confined. Lattice simulations suggest that the critical temperature T_c for the transition in the presence of two light flavors is around 150 MeV. Temperatures in this range are reached in heavy-ion collisions at the Brookhaven AGS (about

$2 + 2$ GeV per nucleon in the center of mass system), CERN SPS (about $10 + 10$ GeV), but only for a very short time. In the near future, the dedicated heavy ion collider RHIC ($100 + 100$ GeV), now under construction in Brookhaven, will allow us to study these conditions in greater detail.

In order to interpret these experiments, we need to understand the properties of hadrons and hadronic matter near and above the phase transition. But before we can hope to accomplish this, we have to understand how the vacuum is rearranged when chiral symmetry is restored. If instantons provide the mechanism for chiral symmetry breaking at $T = 0$, one expects them to play an important role at $T \sim T_c$ as well.

Formally, extending the instanton liquid model to finite temperature is rather straightforward. In Euclidean space, considering $T \neq 0$ corresponds to making the Euclidean time direction periodic. The length of the Euclidean time axis is determined by the inverse temperature, $\tau_{\max} = 1/T$. Finite temperature instantons, i.e. solutions to the classical Yang-Mills equations subject to periodic boundary conditions, are known analytically. These solutions have action $S = 8\pi/g^2$ and topological charge $Q = 1$, independent of T.

It was realized early on that at high temperature instantons should be suppressed (71). Therefore, it was generally assumed that chiral symmetry restoration is a consequence of the disappearance of instantons with higher T. However, more recently it was argued that *below the phase transition* instantons should not be suppressed (72). This idea was confirmed by lattice measurements of the topological susceptibility (73), which found little change in the topological susceptibility for $T < T_c$, and the expected suppression for $T > T_c$. This is consistent with the idea that instanton suppression is a reflection of Debye screening (10), which is a plasma effect.

If instantons do not disappear, then the phase transition has to be caused by a rearrangement of the instanton liquid. It was suggested that chiral-symmetry restoration involves a transition from a random phase below T_c to a correlated phase of instanton–anti-instanton molecules above T_c (74, 75). These molecules correspond to the most symmetric configuration of an instanton–anti-instanton pair on the Matsubara torus. The two instantons are at the same spatial point but separated by half the Matsubara box in time, $\Delta\tau = 1/(2T)$. We have verified that this configuration provides a very large attractive interaction. The effect is maximal when the molecule exactly fits onto the torus, i.e. $4\rho \simeq 1/T$. From the standard value $\rho \simeq 0.33$ fm, we obtain the estimate $T \simeq 150$ MeV, close to the expected transition temperature.

We have studied the phase transition in numerical simulations of the instanton liquid and explored a number of physical consequences (6). The simulations support the basic mechanism outlined above. As an example, Figure 5 shows a typical snapshot of the instanton ensemble below and above the phase transition. Above T_c, we clearly observe the formation of polarized

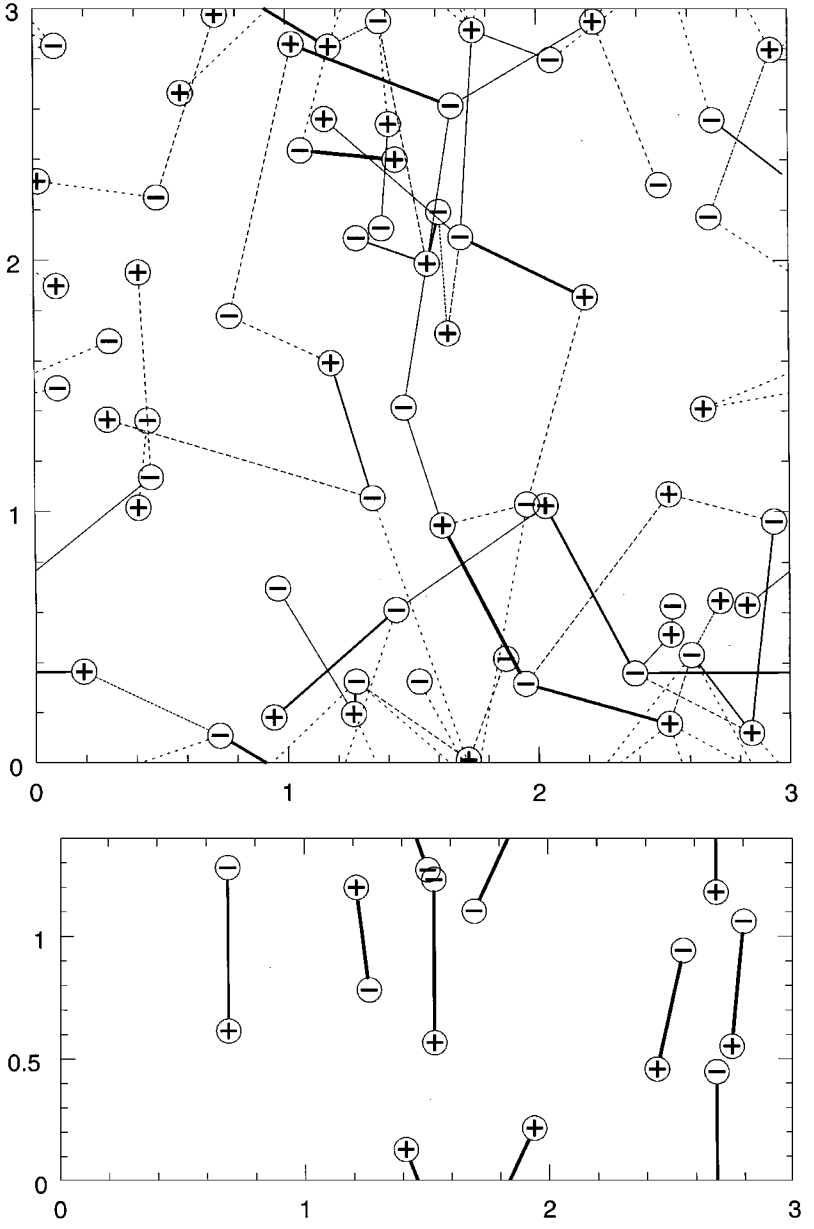

instanton–anti-instanton molecules.[7] In addition to that, many thermodynamic parameters, the spectra of the Dirac operator, the quark condensate, chiral susceptibilities and hadronic correlation functions were calculated (38, 77). The results are consistent with the available lattice data. However, some unexpected results were also found. In particular, there are indications that certain hadronic states (especially scalar and pseudoscalar mesons) survive the phase transition as resonances in the quark continuum.

Phase Structure of QCD-Like Theories

A promising way to understand the role of dynamical quarks in QCD is to study the structure of QCD with more light flavors (in the following we will always fix the number of colors $N_c = 3$). If the number of flavors is too large, $N_f > 33/2$, asymptotic freedom is lost and we get a theory very much like QED, where the charge grows with distance. The largest number of light flavors we can have and still keep asymptotic freedom is $N_f = 16$. In the following, we will try to understand what happens if N_f is gradually reduced (see Figure 6). For large N_f, QCD is in a conformal phase (78). The running coupling constant has an infrared fixed point at $g_*^2/16\pi^2 = -b/b' \ll 1$, where b, b' are the one- and two-loop coefficients of beta function. If N_f is close to 33/2, g_*^2 is small, so the perturbative analysis is reliable. The existence of an infrared fixed point implies that the theory is not only asymptotically free at short distance, but that the coupling freezes at some fixed value before it becomes large. There is no mass gap and correlators decay as powers of the distance. All non-perturbative phenomena (including instantons) are exponentially suppressed, $\exp(-\text{const}/g_*^2)$.

As the number of flavors is decreased the value of the fixed point coupling becomes larger and the fixed point eventually disappears. Lattice simulations of multi-flavor QCD were recently reported in (79). These authors studied QCD with up to 240 flavors. From the sign of the beta function in the weak and strong coupling domains, they confirmed the existence of an infrared fixed point for as few as $N_f = 7$ flavors. Below that point, we expect chiral symmetry breaking and confinement to set in, possibly with a number of intermediate phases such as a non-abelian Coulomb phase, or a phase with chiral symmetry breaking but

[7]The phase transition shows an amusing similarity to the Koesterlitz-Thouless transition (76) in the two-dimensional O(2) sigma model. In this case, the transition connects a low-temperature phase of vortex-antivortex pairs with a high-temperature vortex plasma (note that the two phases are interchanged as compared to QCD).

←

Figure 5 Typical instanton ensembles for $T = 75$ and 158 MeV, from (38). The plots show projections of a four-dimensional $(3\Lambda^{-1})^3 \times T^{-1}$ box into the 3-4 (z axis-imaginary temperature) plane. Instantons and anti-instanton positions are indicated by $+$ and $-$ symbols. The lines show the strength of the fermion hopping matrix elements (bonds).

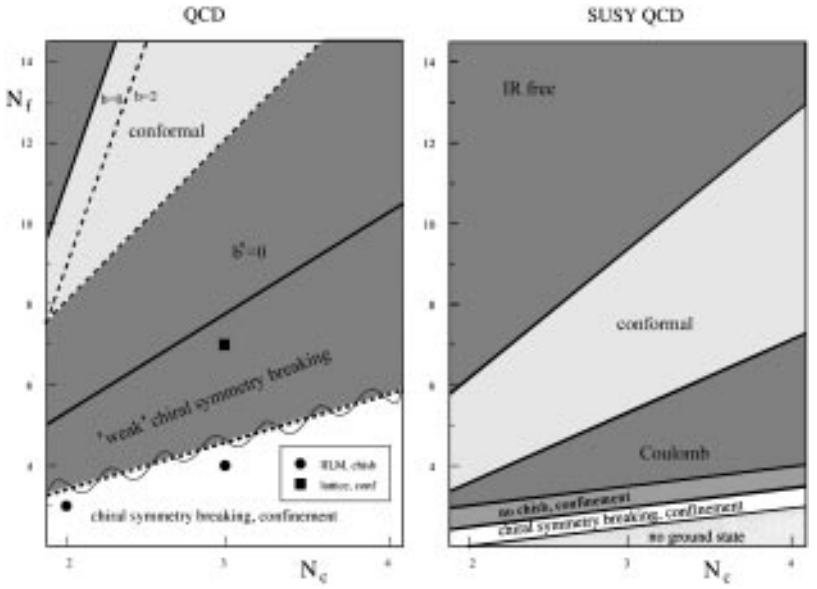

Figure 6 Schematic phase diagram of QCD (a) and supersymmetric QCD (b) as a function of the number of colors N_c and the number of flavors N_f. Squares show points where lattice simulations have found an infrared fixed point and dots denote points in the phase diagram where the instanton ensemble is purely molecular, with unbroken chiral symmetry.

no confinement. Clearly, there remains a lot of work to be done in order to clarify the phase structure of QCD with many flavors.

Known results for the interacting instanton model can be summarized as follows. For $N_f = 2$ we found a second order phase transition at finite temperature. For $N_f = 3$ the transition becomes weakly first order. The transition temperature decreases with increasing N_f and for[8] $N_f \geq 5$ one finds that chiral symmetry is restored even at $T = 0$. This is in agreement with lattice results obtained by the Columbia group (R. Mawhinney, private communication). For $N_f = 4$ they found a dramatic reduction in chiral-symmetry breaking effects as compared to $N_f \leq 3$. In particular, the observed mass splittings $\pi - \sigma, \rho - a_1, N - N^*(1/2^-)$ are much smaller. This suggests that chiral restoration is nearby, similarly to what was found in the instanton calculations.

Now we would like to return to Figure 6, and explain its second part, the phase structure of $N = 1$ SUSY QCD (80). Supersymmetric QCD contains a number

[8]Note that even if chiral symmetry is restored in the instanton liquid simulations, there is still the possibility of weak chiral symmetry breaking due to very large instantons (see the discussion in 4). However, the quark condensate would be much smaller and hard to observe in lattice simulations.

of additional fields, fermions with the color structure of gluons (gluinos) and scalar partners of quarks (squarks). These scalar fields act like the Higgs field in electroweak theory. In particular, the tunneling rate is small if the squark vacuum expectation value is large. Supersymmetric theories have a number of theoretical advantages over ordinary QCD. For example, many perturbative effects cancel and instanton effects are more easily identified. Furthermore, supersymmetry greatly constrains the structure of the effective potential and the phase diagram Figure 6 is completely determined.

In the case of SUSY QCD, the existence of a conformal phase, a Coulomb phase and a chirally broken, confining phase are established. In addition to that, the theory has two unusual phases (presumably absent in QCD): a phase without a stable ground state and a phase with unbroken chiral symmetry but confinement. The instability for $N_f \leq N_c - 1$ is caused by the contribution of instanton–anti-instanton molecules to the vacuum energy (unlike QCD, this contribution can be calculated reliably). Also, it is amusing to note that chiral symmetry is restored at $N_f = N_c + 1$, similar to what was found for QCD in the instanton model.

As mentioned in the introduction, instanton calculations can be checked in even more detail in the case of $N = 2$ supersymmetric QCD. This theory has an additional supersymmetry, and even more fermion and scalar fields. The theory has neither confinement nor chiral symmetry breaking[9] and we will not discuss its phase structure any further.

SUMMARY AND OUTLOOK

With this review, we want to draw attention to a number of recent results in nonperturbative QCD. These developments have helped to identify instantons as a dominant phenomenon connecting the underlying gauge theory to the effective description of QCD at low momenta. The typical instanton size is small, and ρ^{-1} sets the scale that determines both the lower boundary of perturbative QCD and the upper boundary of effective chiral Lagrangians. Instantons provide a microscopic mechanism for chiral symmetry breaking and explain how pointlike "current" quarks become massive and extended "constituent" quarks.

Progress was made possible by two developments. First, a large number of hadronic correlation functions were calculated in the instanton liquid model. These correlators are available both quenched and unquenched, with the instanton induced interaction included to all orders. The results have been compared with both phenomenology and the lattice, showing very good agreement. More

[9]The main interest of $N = 2$ SUSY QCD comes from the fact that the theory becomes confining if slightly perturbed to $N = 1$ QCD. The confinement mechanism is monopole condensation.

accurate comparisons will be possible as soon as more detailed (unquenched!) lattice calculations become available. In particular, at some point one should be able to see the effects of phenomena not included in the instanton model, such as confinement.

Second, there has been a lot of progress in direct studies of instantons on the lattice. There are data concerning the total density, the typical size, the size distribution and correlations between instantons. Furthermore, there are detailed studies of the mechanism of $U(1)_A$ violation, and of the behavior of correlation functions under cooling. Recent investigations have begun to focus on many interesting questions, like correlations of instantons with monopoles.

Let us briefly summarize the basic picture of the QCD vacuum that has emerged from the instanton liquid model. The main point is that the gauge fields are very inhomogeneous. Strong, polarized fields are concentrated in small regions of space-time. Quark fields, on the other hand, cannot be localized inside instantons. In order to have a finite tunneling probability, quarks have to be exchanged between instantons and anti-instantons. This difference leads to significant differences between gluonic and fermionic correlation functions. Gluonic correlators are short-range and the mass scale for glueballs is significantly larger than that for mesons. In addition to that, the fact that the gluonic fields are strongly polarized leads to large spin splittings in both glueballs and light mesons.

While the instanton liquid picture works well, there are still open questions concerning its theoretical justification. We still do not understand why large-size instantons are suppressed. On a phenomenological level we can account for this fact by including a repulsive core in the instanton–anti-instanton interaction, but the physical nature of this interaction has not been clarified. The problem is related to the interplay between instantons and high-order perturbative contributions. In this context, studies of SUSY gauge theories might be useful, because perturbative contributions are simpler.

We have also discussed implications of the instanton liquid model for the behavior of QCD at finite temperature. The most important development in this field has been the realization that instantons are not suppressed at temperatures $T \leq T_c$, but only disappear at significantly higher temperatures. This implies that there are a number of non-perturbative effects caused by instantons even in the plasma phase. We have argued that the transition is caused by a rearrangement of the instanton liquid, going from a (dominantly) random phase at low temperature to a correlated phase of instanton–anti-instanton molecules at high temperature. This mechanism provides the correct scale for the transition temperature, and gives predictions for the phase diagram, the critical behavior of mesonic susceptibilities, etc, that are in agreement with what is known from the lattice.

This picture of the chiral phase transition has important consequences. If instantons are still present at $T > T_c$ (although bound into topologically neutral pairs) they will contribute to the interaction between quarks and the equation of state. This means that instanton effects might play an important role in the quark gluon plasma at moderate temperatures $T = (1-2)T_c$. This is the regime of temperatures that we might hope to reach at the heavy-ion accelerators currently operating or under construction. We have begun to explore some of these consequences in more detail, in particular the behavior of spatial and temporal correlation functions across the transition region. While spacelike screening masses essentially agree with the results of lattice calculations, interesting phenomena are seen in temporal correlation functions. Here we found hints that some hadronic modes might survive in the high-temperature phase. Clearly, much work remains do be done in order to improve our understanding of the high-temperature phase.

And, finally, it is important to find out to what extent the instanton liquid picture can be extended to other QCD-like theories. In particular, we have speculated about the phase structure of cold QCD as a function of the number of colors and flavors. Other theories might also be considered, with exact results available for supersymmetric gauge theories providing important guidance. Many exciting discoveries are waiting for us on the way.

Literature Cited

1. Y. Nambu and G. Jona-Lasinio. Phys. Rev., 122:345, 1961.
2. E. V. Shuryak. *Phys. Lett.*, 107B:103, 1981.
3. H. Georgi and A. Manohar. *Nucl. Phys.*, B234:189, 1984.
4. T. Schäfer and E. V. Shuryak. *Rev. Mod. Phys.*, to appear 1997.
5. E. V. Shuryak. *Nucl. Phys.*, B203:93, 1982.
6. T. Schäfer and E. V. Shuryak. *Phys. Rev. Lett.*, 75:1707, 1995.
7. M. Feurstein, E. M. Ilgenfritz, M. Muller-Preussker, and S. Thurner. 1996.
8. M. C. Chu, J. M. Grandy, S. Huang, and J. W. Negele. *Phys. Rev.*, D49:6039, 1994.
9. T. DeGrand, R. L. Jaffe, K. Johnson, and J. Kiskis. *Phys. Rev.*, D12:2060, 1975.
10. E. V. Shuryak. *Phys. Lett.*, B79:135, 1978.
11. A. A. Belavin, A. M. Polyakov, A. A. Schwartz, and Yu. S. Tyupkin. *Phys. Lett.*, 59B:85, 1975.
12. R. Jackiw and C. Rebbi. *Phys. Rev. Lett.*, 37:172, 1976.
13. C. G. Callan, R.F. Dashen, and David J. Gross. *Phys. Lett.*, 63B:334, 1976.
14. A. M. Polyakov. *Nucl. Phys.*, B120:429, 1977.
15. G. 't Hooft. *Phys. Rev.*, D14:3432, 1976.
16. C. G. Callan, R. Dashen, and D. J. Gross. *Phys. Rev.*, D17:2717, 1978.
17. M. A. Shifman, A. I. Vainshtein, and V. I. Zakharov. *Nucl. Phys.*, B147:385, 448, 1979.
18. V. A. Novikov, M. A. Shifman, A. I. Vainshtein, and V. I. Zakharov. *Nucl. Phys.*, B191:301, 1981.
19. B. V. Geshkenbein and B. L. Ioffe. *Nucl. Phys.*, B166:340, 1980.
20. E. V. Shuryak. *Nucl. Phys.*, B214:237, 1983.
21. E. Witten. *Nucl. Phys.*, B149:285, 1979.
22. G. Veneziano. *Nucl. Phys.*, B159:213, 1979.
23. E. V. Shuryak. *Nucl. Phys.*, B198:83, 1982.
24. E. M. Ilgenfritz and M. Muller-Preussker.

Nucl. Phys., B184:443, 1981.
25. D. I. Diakonov and V. Yu. Petrov. *Nucl. Phys.*, B245:259, 1984.
26. D. I. Diakonov and V. Yu. Petrov. *Nucl. Phys.*, B272:457, 1986.
27. E. V. Shuryak. *Nucl. Phys.*, B302:559, 574, 599, 1988.
28. P. Woit. *Phys. Rev. Lett.*, 51:638, 1983.
29. K. Ishikawa, G. Schierholz, H. Schneider, and M. Teper. *Phys. Lett.*, 128B:309, 1983.
30. I. A. Fox, J. P. Gilchrist, M. L. Laursen, and G. Schierholz. *Phys. Rev. Lett.*, 54:749, 1985.
31. M. Teper. *Phys. Lett.*, 162B:357, 1985.
32. E. V. Shuryak and J. J. M. Verbaarschot. *Nucl. Phys.*, B410:55, 1993.
33. T. Schäfer, E. V. Shuryak, and J. J. M. Verbaarschot. *Nucl. Phys.*, B412:143, 1994.
34. T. Schäfer and E. V. Shuryak. *Phys. Rev.*, D54:1099, 1996.
35. E. V. Shuryak. *Rev. Mod. Phys.*, 65:1, 1993.
36. M. C. Chu, J. M. Grandy, S. Huang, and J. W. Negele. *Phys. Rev. Lett.*, 70:225, 1993.
37. E. V. Shuryak and J. J. M. Verbaarschot. *Phys. Rev.*, D52:295, 1995.
38. T. Schäfer and E. V. Shuryak. *Phys. Rev.*, D53:6522, 1996.
39. J. Hoek, M. Teper, and J. Waterhouse. *Nucl. Phys.*, B288:589, 1987.
40. A. Hasenfratz, T. DeGrand, and D. Zhu. hep-lat/9604018, 1996.
41. N. Seiberg and E. Witten. *Nucl. Phys.*, B426:19, 1994.
42. D. Finnel and P. Pouliot. *Nucl. Phys.*, B453:225, 1995.
43. K. Ito and N. Sasakura. *Phys. Lett.*, B382:95, 1996.
44. N. Dorey, V. V. Khoze, and M. P. Mattis. *Phys. Rev.*, D54:2921, 1996.
45. H. Aoyama, T. Harano, M. Sato, and S. Wada. Preprint, hep-th/9607076, 1996.
46. M. C. Chu, J. M. Grandy, S. Huang, and J. W. Negele. *Phys. Rev.*, D 48:3340, 1993.
47. R. Rajaraman. *Solitons and Instantons.* North Holland, Amsterdam, 1982.
48. M. Shifman. *Instantons in Gauge Theories.* World Scientific, Singapore, 1994.
49. D. I. Diakonov and V. Yu. Petrov. *Phys. Rev.*, D50:266, 1994.
50. M. A. Shifman, A. I. Vaishtein, and V. I. Zakharov. *Phys. Lett.*, B76:971, 1978.
51. E. Witten. *Nucl. Phys.*, B156:269, 1979.
52. M. Feuerstein, H. Markum, and S. Thurner. Preprint, University of Vienna, 1997.
53. C. Michael and P. S. Spencer. *Phys. Rev.*, D52:4691, 1995.
54. E. V. Shuryak. *Phys. Rev.*, D52:5370, 1995.
55. S. L. Adler. *Phys. Rev.*, 177:2426, 1969.
56. J. S. Bell and R. Jackiw. *Nuovo Cim.*, A60:47, 1969.
57. V. N. Gribov. Preprint, KFKI-1981-66, Budapest, 1981.
58. M. A. Shifman. *Sov. Phys. Usp.*, 32:289, 1989.
59. G. 't Hooft. *Phys. Rev. Lett.*, 37:8, 1976.
60. M. A. Shifman, A. I. Vainshtein, and V. I. Zakharov. *Nucl. Phys.*, B163:46, 1980.
61. U. Vogl and W. Weise. *Progr. Nucl. Part. Phys.*, 27:195, 1991.
62. S. P. Klevansky. *Rev. Mod. Phys.*, 64:649, 1992.
63. T. Hatsuda and T. Kunihiro. *Phys. Rep.*, 247:221, 1994.
64. D. I. Diakonov. International School of Physics, Enrico Fermi, Course 80, Varenna, Italy, 1995.
65. T. Banks and A. Casher. *Nucl. Phys.*, B169:103, 1980.
66. M. Hutter. Preprint, hep-ph/9501245, 1995.
67. M. Kacir, M. Prakash, and I. Zahed. Preprint, hep-ph/9602314, 1996.
68. S. Chernyshev, M. A. Nowak, and I. Zahed. Preprint, hep-ph/9510326, 1995.
69. C. G. Callan, R. F. Dashen, and D. J. Gross. *Phys. Rev.*, D18:4684, 1978.
70. F. de Forcrand and K.-F. Liu. *Phys. Rev. Lett.*, 69:245, 1992.
71. R. D. Pisarski and L. G. Yaffe. *Phys. Lett.*, B97:110, 1980.
72. E. V. Shuryak and M. Velkovsky. *Phys. Rev.*, D50:3323, 1994.
73. M. C. Chu and S. Schramm. *Phys. Rev.*, D51:4580, 1995.
74. E.-M. Ilgenfritz and E. V. Shuryak. *Phys. Lett.*, B325:263, 1994.
75. T. Schäfer, E. V. Shuryak, and J. J. M. Verbaarschot. *Phys. Rev.*, D51:1267, 1995.
76. J. M. Koesterlitz and D. J. Thouless. *J. Phys.*, C6:118, 1973.
77. E. Shuryak and M. Velkovsky. Preprint, hep-ph/9603234, 1996.
78. T. Banks and A. Zaks. *Nucl. Phys.*, B82:196, 1982.
79. Y. Iwasaki, K. Kanaya, S. Kaya, S. Sakai, and T. Yoshie. *Z. Phys.*, C71:343, 1996.
80. N. Seiberg. *Phys. Rev.*, D49:6857, 1994.

Annual Review of Nuclear and Particle Science
Volume 47, 1997

CONTENTS